AB

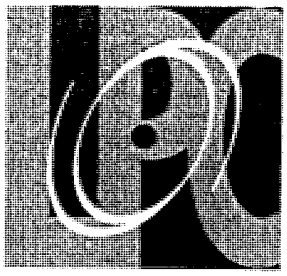

Laboratoire de Physique Corpusculaire
de Clermont-Ferrand

Experimental Review on $|V_{ub}|$

Philippe ROSNET

Laboratoire de Physique Corpusculaire
de Clermont-Ferrand
IN2P3/CNRS - Université Blaise Pascal
63177 AUBIERE CEDEX France

Presented at the

XXIX International Conference on High Energy Physics
ICHEP'98
Vancouver, Canada - July 23-29, 1998

PCCF RI 9806

EXPERIMENTAL REVIEW ON $|V_{ub}|$

Philippe Rosnet

Laboratoire de Physique Corpusculaire de Clermont-Ferrand
Université Blaise Pascal / IN2P3 - CNRS
E-mail: rosnet@clermont.in2p3.fr

This paper presents an experimental review of the Cabibbo-Kobayashi-Maskawa (CKM) matrix element V_{ub}. From the data samples recorded by the $\Upsilon(4S)$ and the Z resonance experiments, both inclusive and exclusive analysis of the charmless semileptonic decays of b hadrons $b \to u l \nu_l$ give measurements of $|V_{ub}|$. Combining all the results, the value obtained is: $|V_{ub}| = (3.56 \pm 0.55) \times 10^{-3}$.

1 Introduction

The quarks are mixed under the weak interaction and the phenomena is described by the CKM matrix [1]:

$$V_{CKM} = \begin{pmatrix} V_{ud} & V_{us} & V_{ub} \\ V_{cd} & V_{cs} & V_{cb} \\ V_{td} & V_{ts} & V_{tb} \end{pmatrix} .$$

Using the parametrisation of Wolfenstein [2], one gets:

$$V_{CKM} \approx \begin{pmatrix} 1 - \frac{\lambda^2}{2} & \lambda & A\lambda^3(\rho - i\eta) \\ -\lambda & 1 - \frac{\lambda^2}{2} & A\lambda^2 \\ A\lambda^3(1 - \rho - i\eta) & -A\lambda^2 & 1 \end{pmatrix} ,$$

valid up to $\mathcal{O}(\lambda^4)$.

The unitarity of the matrix leads to $V_{ud}V_{ub}^* + V_{cd}V_{cb}^* + V_{td}V_{tb}^* = 0$, represented by the unitarity triangle on figure 1. One of these sides is characterised by the element V_{ub}. In the framework of the Standard Model, the understanding of the CP violation requires a detailed study of the whole triangle, namely the sides and the angles.
In this optic, a precise measurement of V_{ub} is required.

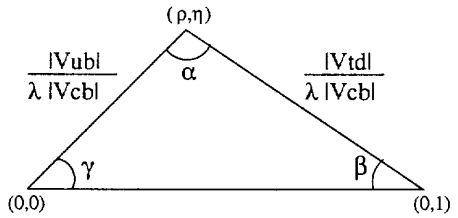

Figure 1: Unitarity triangle in the complex plane (ρ, η).

2 Semileptonic b → u decays

From a theoretical and experimental point of view, only semileptonic $b \to u$ transitions are studied to extract $|V_{ub}|$ (see Fig. 2). In practice, two approaches can be used to derive the matrix element from the measurement of the branching ratio:

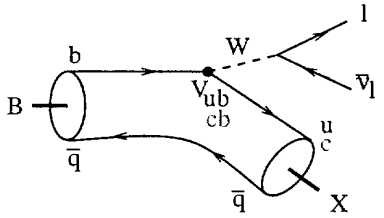

Figure 2: Semileptonic B decay, where X represent the hadronic system produced.

- In the case of exclusive final states (X_u = π or ρ or η ...), the experimental reconstruction is relatively easy, but the bad knowledge of the form factors implies a large model dependence.
- In the inclusive study, where all the final states are taken into account (X_u = π, $\eta^{(\prime)}$, ρ, ω, ..., $\pi\pi$, $\pi\pi\pi$, ...), the experimental reconstruction is more difficult, but the theoretical prediction is quite accurate [3] :

$$|V_{ub}| = 0.00465 \sqrt{\frac{Br(b \to X_u l \nu_l)}{0.002}} \sqrt{\frac{1.55\text{ps}}{\tau_b}} (1 \pm 0.025_{\text{pert}} \pm 0.03_{m_b}) ,$$

which corresponds to 4 % of precision.

Unfortunately, the $b \to c$ transitions are dominant by approximatively two orders of magnitude, with X_c = D, D^*, D^{**}, $D^*\pi$, ... Therefore a good discrimination between the two types of decays ($b \to u$ and $b \to c$) is needed.

Inclusively, the $b \to X_u l \nu_l$ transitions are characterised by a low hadronic mass spectrum (M_X) and a high lepton energy end-point in the centre of mass of the b hadron (E_l^*), see Fig. 3. With a perfect reconstruction and 100 % of efficiency, we can select around 90 % of $b \to u$ decays with the M_X spectrum and only 10 % from

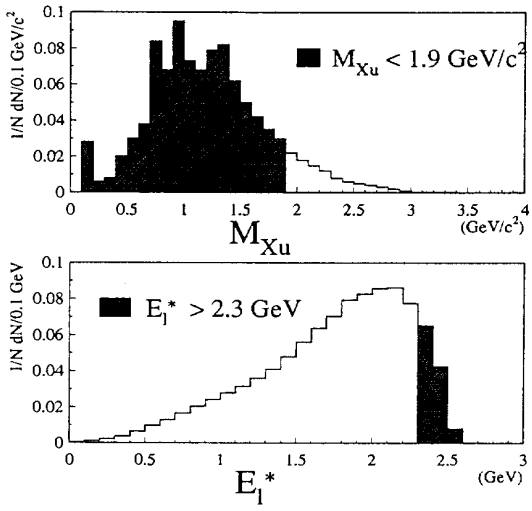

Figure 3: Hadronic mass (upper plot) and lepton energy (lower plot) for inclusive $b \to X_u l\nu_l$ decays. For each plot, the hatched part shows the region forbidden to the $b \to X_c l\nu_l$ decays.

the E_l^* distribution, illustrating the advantage to use the properties of the hadronic system.

At the $\Upsilon(4S)$, the two B mesons are produced almost at rest and their decay products are completely mixed. In this case, it is difficult to distinguish the particles coming from the two B's. On the other hand, at LEP, the situation is different because the two b quarks are boosted and then the decay products of the b hadrons are well separated. In these conditions, it is possible to reconstruct inclusively the hadronic system coming from the semileptonic b decay.

3 Υ(4S) experiments

3.1 Inclusive studies

The first evidence of $b \to u l\nu_l$ transitions has been done, next to the $e^+e^- \to \Upsilon(4S) \to B\bar{B}$ accelerators, by observing an excess of events in the lepton energy spectrum above the $b \to c$ end-point. ARGUS (at DORIS) and CLEO (at CESR) experiments [5] give the following values of the ratio $|V_{ub}|/|V_{cb}|$:

$$\text{ARGUS} \to \frac{|V_{ub}|}{|V_{cb}|} = 0.130 \pm 0.017_{stat+syst} \pm 0.047_{model}$$
$$\text{CLEO} \to \frac{|V_{ub}|}{|V_{cb}|} = 0.080 \pm 0.008_{stat+syst} \pm 0.021_{model}$$

With the value [4] $|V_{cb}| = 0.0392 \pm 0.0027$, one gets the values of $|V_{ub}|$ given in table 5 (called respectively ARGUS and CLEO end-point).

3.2 Exclusive studies

An other way to observe $b \to u l\nu_l$ transition consists to reconstruct a B meson in a specific channel. First, upper limits on the vector modes $\rho l\nu_l$ and $\omega l\nu_l$ have been given by CLEO [6], and afterwards a measurement of the exclusif branching ratio have been performed from the excess of events observed in the reconstructed B mass [6]:

$$\begin{cases} Br(B^0 \to \pi^+ l^- \bar{\nu}_l) = (1.8 \pm 0.4_{stat} \pm 0.3_{syst} \\ \qquad\qquad \pm 0.2_{model}) \times 10^{-4} \\ Br(B^0 \to \rho^+ l^- \bar{\nu}_l) = (2.5 \pm 0.4_{stat} \pm^{0.5}_{0.7 syst} \\ \qquad\qquad \pm 0.5_{model}) \times 10^{-4} \end{cases},$$

where the first error is statistical, the second is from the estimation of the residual background and the third is from the modelling of the signal.
By combining these results, the value of $|V_{ub}|$ is determined, see table 5 (called CLEO exclusif).

A new exclusive study has been done by the CLEO experiment [7], with $N(e^+e^- \to \Upsilon(4S) \to B\bar{B}) = 3.3 \times 10^6$ (compare to 2.8×10^6 in the previous analysis). The analysis concerns the vector mode $B \to \rho(\to \pi\pi) l\nu_l$ and $B \to \omega(\to \pi\pi\pi) l\nu_l$, with a lepton momentum greater than 1.7 GeV/c, while the pseudo-scalar mode $B \to \pi l\nu_l$ is used only as a check and to estimate its contribution as background in the ρ channel. Assuming the isospin symmetry $\Gamma_{\rho^\pm} = 2\Gamma_{\rho^0} = 2\Gamma_\omega$, the fraction of $B^0 \to \rho^+ l^- \bar{\nu}_l$ is fitted in the plane $M_{\pi\pi(\pi)}$ versus ΔE (see Fig. 4), where $\Delta E = E_{\pi\pi(\pi)} + E_l + |\vec{p}_{miss}| - E_{beam}$. In the fit, the lepton energy is divided in three regions: $1.7 < E_l < 2.0$ GeV poor in $b \to u$ and used to normalized the background, $2.0 < E_l < 2.3$ GeV mixing $b \to u$ and $b \to c$ decays, and $2.3 < E_l < 2.7$ GeV rich in $b \to u$ transitions. The result

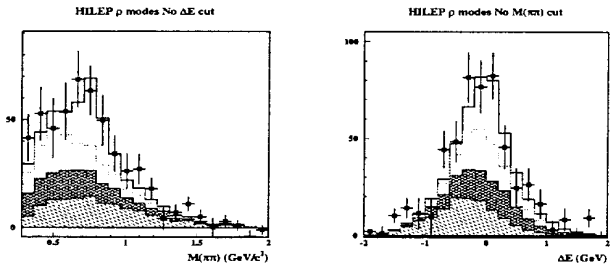

Figure 4: $M_{\pi\pi}$ (left plot) and ΔE (right plot) for the ρ channel in the lepton energy range $2.3 < E_l < 2.7$ GeV. For each plot, the squares represent the data; and the histograms the Monte Carlo with the signal (in white), the cross-feed components of the signal (dotted line), the background from $b \to u l\nu_l$ non-signal modes (double-hatched region), and the background from $b \to c l\nu_l$ (single-hatched region).

Table 1: Result of the branching ratio for the $B^0 \to \rho^+ l^- \bar{\nu}_l$ obtained by CLEO with different models, where the first error is statistical while the second comes from the model itself.

Model	$Br(B^0 \to \rho^+ l^- \bar{\nu}_l) \times 10^4$
Quark model (average)	$2.7 \pm 0.4 \pm 0.4$
Lattice (UKQCD)	$2.8 \pm 0.4 \pm 0.1$
LCSR (Ball/Braun)	$3.2 \pm 0.5 \pm 0.4$
Ligeti/Wise + E791	2.5 ± 0.4

of the fit gives:

$$Br(B^0 \to \rho^+ l^- \bar{\nu}_l) = (2.8 \pm 0.4_{stat} \pm 0.4_{syst} \pm 0.6_{model}) \times 10^{-4} ,$$

where the modelling error comes from the dispersion of the result with respect to the different exclusive models used [7], see table 1.

The excess of events observed after the fit (see Fig. 5) and the efficiency for each channel, in the region $2.0 < E_l < 2.7\,\mathrm{GeV}$, are:

$$\begin{cases} \rho^{\pm} \longrightarrow (116 \pm 18) \text{ events with } \epsilon = 3.9\,\% \\ \rho^0 \longrightarrow (114 \pm 17) \text{ events with } \epsilon = 9.1\,\% \\ \omega \longrightarrow (53 \pm 8) \text{ events with } \epsilon = 3.7\,\% \end{cases} .$$

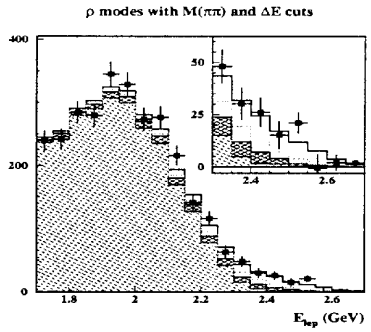

Figure 5: Lepton energy for the ρ mode after the cuts: $|M_{\pi\pi} - M_\rho| \leq 150\,\mathrm{MeV/c^2}$ and $|\Delta E| \leq 500\,\mathrm{MeV}$. The differents contribution are the same than for the previous figure.

From the measured branching ratio, the value of $|V_{ub}|$ (largely statistically independent from the previous analysis) given in table 5 (called CLEO vector) is extracted.

4 Z experiments

For all the $\Upsilon(4S)$ results, the modelling of the $b \to u l \nu_l$ transitions is the dominant error on $|V_{ub}|$. It comes from the fact that in the exclusive searches the prediction of the associated form factors suffers from large uncertainties, and in the end-point studies only a small part of the lepton energy phase space is considered. The idea is then to develop at the Z pole an inclusive analysis including the information provided by the hadronic system, which is in theory very powerful (see Fig. 3).

4.1 ALEPH measurement

The ALEPH study [8] is based on 3.6×10^6 $Z \to q\bar{q}$ events. The principle of the analysis is the following:

- A lepton (electron or muon) is identified with a momentum greater than $3.0\,\mathrm{GeV/c}$. A b-tag is applied on the opposite hemisphere, the neutrino is reconstruct with the help of the missing momentum of the event ($\vec{p}_{\nu_l} = \vec{p}_{miss}$ and $E_{\nu_l} = |\vec{p}_{\nu_l}|$), and the hadronic system X is selected by using two neural networks (one for charged tracks and one for photons) to discriminate the b tracks with respect to the fragmentation tracks. All the decay products of the b hadrons (l, ν_l and X) allow to calculate its four-momentum.

- Afterwards, discriminating variables between $b \to u l \nu_l$ and $b \to c + l$ decays (direct $b \to c l \nu_l$, cascade $b \to c \to l$, $c \to l$, $b \to \bar{c} \to l$, $J/\psi \to l$, miss-identifications, ...) are constructed in the centre of mass of the b hadron: invariant mass, sphericity, lepton energy, ... 20 such variables are combined inside a neural network called NN_{bu} to improve the separation between $b \to u$ and $b \to c$ transitions, see Fig. 6. The advantage of this method is to have similar efficiency for neutral and charged modes as explained by figure 6.

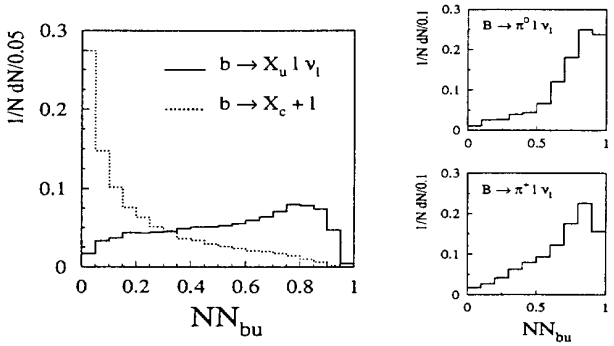

Figure 6: Neural network output NN_{bu} (left plot) to discriminate the $b \to u l \nu_l$ transitions from the $b \to c + l$ background. NN_{bu} for the $B \to \pi l \nu_l$ modes (right plots): for the π^0 (upper plot) and the $\pi^{\pm}$ (lower plot) channels.

- Finally the shape of the neural network NN_{bu} is fitted to extract $Br(b \to X_u l\nu_l)$.

Figure 7 shows the comparison between data and simulation for NN_{bu}. An excess of 303 ± 88 events appears in the signal region ($NN_{bu} > 0.6$) which is attributed to $b \to X_u l\nu_l$ transitions. A fit to this part of the neural

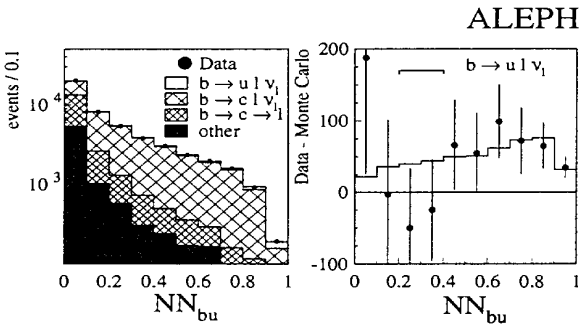

Figure 7: Comparison of the neural network output NN_{bu} (left plot) for data (points) and the simulation (histograms) with the signal, the direct $b \to c l\nu_l$ background, the cascade $b \to c \to l$ and the other sources of leptons ($c \to l$, $b \to \bar{c} \to l$, $J/\psi \to l$, miss-identifications, ...). Difference data - Monte Carlo without $b \to u$ transitions (right plot).

network (corresponding to an efficiency of 50 % for the signal) gives the inclusive branching ratio:

$$Br(b \to X_u l\nu_l) = (1.73 \pm 0.55_{stat} \pm 0.51_{syst} \pm 0.21_{model}) \times 10^{-3} ,$$

where the $b \to c + l$ systematic errors come from four main sources and are summarised in table 2.
In this analysis, the signal is described with an hybrid model [8] (see Fig. 3) by taking resonant states (25 %) at low hadronic recoil $E_u < 1.6$ GeV with ISGW2 model [8] and multi-body states (75 %) at large recoil $E_u \geq 1.6$ GeV with the DSU model [8] (Dikeman-Shifman-Uraltsev). The corresponding systematic errors are estimated by varing the different parameters of the model [8]. The small error obtained (see table 2) is due to the relatively small sensitivity of the neural network output to the modelling, as explained in figure 8.

Several checks were made to confirm the evidence of inclusive $b \to X_u l\nu_l$ transitions in this analysis: by comparing the NN_{bu} output of Data and Monte Carlo for selected $b \to X_c l\nu_l$ decays; by checking the stability of the result with respect to the fit procedure; by studying the effect of the variables used; and by searching for an evidence of signal for $NN_{bu} > 0.9$ with vertexing method, in the $M_{Xl\nu_l}$ distribution, and by a scan of the events (see Ref. [8] for more details).

Table 2: Systematic errors on the branching ratio $Br(b \to X_u l\nu_l)$ for the ALEPH analysis.

Source of error	$\Delta Br(b \to X_u l\nu_l)$
b hadron production	$\pm 0.16 \times 10^{-3}$
b hadron decay	$\pm 0.31 \times 10^{-3}$
c hadron decay	$\pm 0.37 \times 10^{-3}$
lepton identification	$\pm 0.08 \times 10^{-3}$
Hybrid model parameter	$\pm 0.08 \times 10^{-3}$
Exclusive model	$\pm 0.05 \times 10^{-3}$
inclusive model	$\pm 0.18 \times 10^{-3}$
Λ_b modelling	$\pm 0.04 \times 10^{-3}$

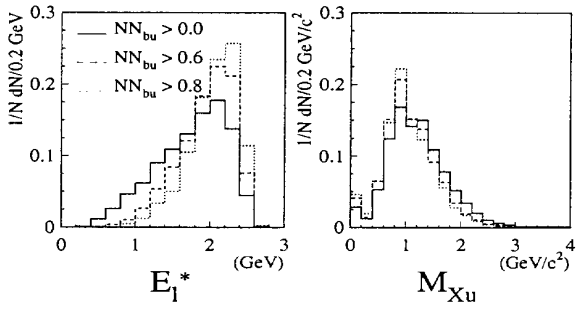

Figure 8: Lepton energy (left plot) and invariant mass (right plot) generated for the $b \to X_u l\nu_l$ transitions for three different cuts on NN_{bu}.

Finally, with the help of theoretical predictions [3], one obtains the result of $|V_{ub}|$ presented in the table 5 (called ALEPH inclusif).

4.2 DELPHI measurement

The DELPHI experiment has presented in the conference a new inclusive analysis [9] based on 2.8×10^6 hadronic Z events. All the decay products of the b hadron: the hadronic system X, the lepton l and the neutrino ν_l are reconstructed; and the background coming from the $b \to c + l$ decays is suppressed with cuts like $E_{Xl} > 12$ GeV and $M_{Xl} > 2.0\,\mathrm{GeV/c^2}$. Then, two samples are defined by using the vertexing conditions of the lepton with respect to the b decay vertex and with the presence of kaon candidates in the lepton hemisphere. Figure 9 shows the reconstructed invariant mass M_X for the $b \to u$ depleted and enriched samples. By cutting at $M_X = 1.6\,\mathrm{GeV/c^2}$ in the two samples, four sub-samples are defined. Then a fit of the reconstructed lepton energy in the b hadron rest frame E_l^* is done simultaneously in the four sub-samples to determine the ratio $|V_{ub}|/|V_{cb}|$. The result obtained

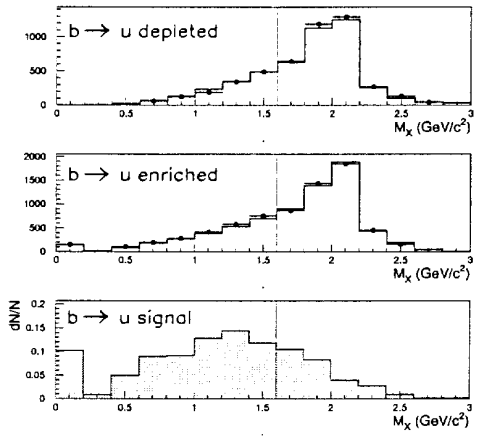

Figure 9: Comparison of the hadronic invariant mass M_X between the Data (point) and the simulation (histogram) for the $b \to u$ depleted sample (upper plot) and the $b \to u$ enriched sample (middle plot). The lower plot shows the distribution for $b \to u$ simulated events.

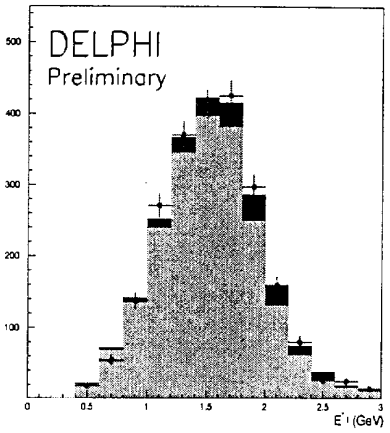

Figure 10: Lepton energy E_l^* for the $b \to u$ enriched sample with $M_X < 1.6\,\mathrm{GeV/c^2}$. The points represent the Data while the histograms the simulation contributions with the signal (in dark) and the $b \to c + l$ background (in light).

Table 3: Systematic errors on the ratio $|V_{ub}|/|V_{cb}|$ for the DELPHI analysis.

Source of error	$\Delta\|V_{ub}\|/\|V_{cb}\|$
b hadron production	± 0.0052
b hadron decay	± 0.0083
c hadron decay	± 0.0065
detector effects	± 0.0101
Signal efficiency	± 0.0012
m_b	± 0.0057
$< p_b^2 >$	± 0.0010
b kinematic model	± 0.0010
Hadronisation model	± 0.0060

is:

$$\frac{|V_{ub}|}{|V_{cb}|} = 0.104 \pm 0.012_{stat} \pm 0.015_{syst} \pm 0.009_{model} \ ,$$

where the error are summarised in table 3. After the fit, the excess of events in the lepton energy spectrum (see Fig. 10) is 205 ± 56 for the $b \to u$ enriched sample with $M_X < 1.6\,\mathrm{GeV/c^2}$ (with 11.2 % of signal efficiency).

With the value of $|V_{cb}|$ given in Ref.[4], one obtains the value of $|V_{ub}|$ given in table 5 (called DELPHI inclusif).

4.3 L3 measurement

An other new inclusive study[10] was presented by the L3 experiment with 1.8×10^6 $Z \to q\bar{q}$ events. The procedure of the analysis is similar to the ALEPH one, except that only the two most energetic tracks of the lepton hemisphere are selected to reconstruct the hadronic system. Then discriminating variables based on the lepton and these two tracks are built (see Fig. 11). A total of 8 such

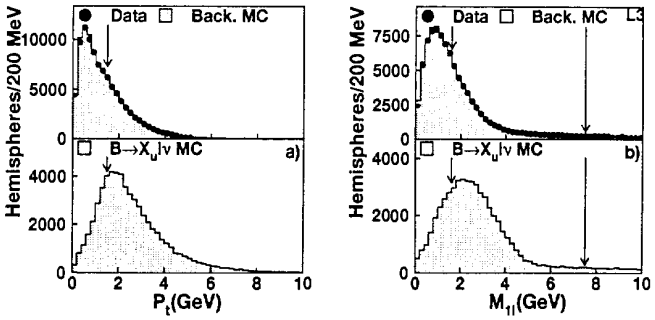

Figure 11: Lepton transverse momentum with respect to the jet axis (left plots), and invariant mass between the lepton and the most energetic track (right plots). For each variable, the upper plot show a comparison between the Data (point) and the background simulation (histogram), while the lower plot the expected signal. The arrows indicate the cuts applied on the variables.

variables are used to reduce the background by a factor 160. Finally, the number of remaining events is used to determined the inclusive branching ratio. The excess of 81 events observed over 576 Data (with 1.5 % of signal efficiency) leads to the result:

$$Br(b \to X_u l \nu_l) = (3.3 \pm 1.0_{stat} \pm 1.66_{syst} \pm 0.55_{model}) \times 10^{-3} \ ,$$

Table 4: Systematic errors on the branching ratio $Br(b \to X_u l \nu_l)$ for the L3 analysis.

Source of error	$\Delta Br(b \to X_u l \nu_l)$
b hadron production	$\pm 0.68 \times 10^{-3}$
b hadron decay	$\pm 1.42 \times 10^{-3}$
detector effects	$\pm 0.52 \times 10^{-3}$
MC statistics	$\pm 0.06 \times 10^{-3}$
Exclusive π rate	$\pm 0.19 \times 10^{-3}$
lepton spectrum	$\pm 0.04 \times 10^{-3}$
π spectrum	$\pm 0.27 \times 10^{-3}$
Λ_b rate	$\pm 0.43 \times 10^{-3}$

where the errors are given in table 4. In this analysis, the signal is described by the ACCMM model [10] (with $p_f = 298\,\mathrm{MeV/c}$ and $m_u = 150\,\mathrm{MeV/c^2}$), except for the $B \to \pi l \nu_l$ channel where an exclusive approach is used (Burdman-Kambor model [10]). As shown in figure 12, a large fraction of the phase space is considered by the analysis explaining the small modelling error.

The cuts on each variable have been changed to check

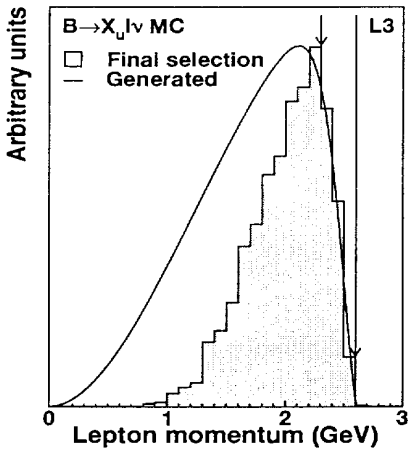

Figure 12: Comparison of the lepton momentum between the generated (line) and selected (histogram) $b \to X_u l \nu_l$ events. To compare the arrows define the range considered by the end-point analysis of CLEO.

the stability of the result. Furthermore, the 8 variables have been combined inside a neural network and the analysis redone, see Fig. 13. The result obtained is in good agreement with the previous one.

Finally, the value of the matrix element $|V_{ub}|$ is determined with the help of the theoretical prediction [3], see table 5 (called L3 inclusif).

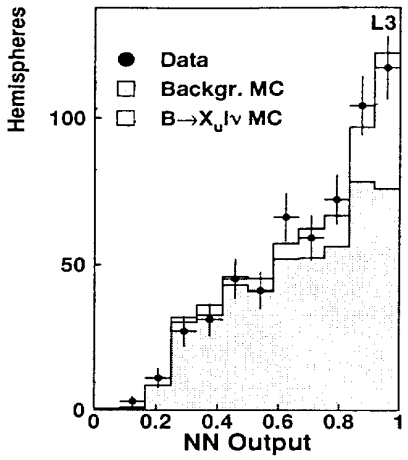

Figure 13: Comparison of the neural network output between the Data (points) and the simulation (histograms) with the signal and background contributions.

Table 5: Summary of all the values of the CKM matrix element $|V_{ub}|$.

Experimental result	$\|V_{ub}\|$ with statistical, systematic and modelling errors ($\times 10^3$)
ARGUS end-point	$5.1 \pm 0.6 \pm 0.2 \pm 1.8$
CLEO end-point	$3.1 \pm 0.2 \pm 0.3 \pm 0.8$
CLEO exclusif	$3.3 \pm 0.2 \pm^{0.3}_{0.4} \pm 0.7$
CLEO vector	$3.2 \pm 0.3 \pm^{0.2}_{0.3} \pm 0.6$
ALEPH inclusif	$4.16 \pm 0.70 \pm 0.64 \pm 0.31$
DELPHI inclusif	$4.08 \pm 0.47 \pm 0.69 \pm 0.35$
L3 inclusif	$6.0 \pm 0.9 \pm 1.6 \pm 0.6$

5 Comparison and discussion

In summary, seven values of the CKM matrix element $|V_{ub}|$ are now available and presented in table 5.

An average value, obtained with a blue technique (consisting to minimise the total error), gives the following result:

$$|V_{ub}| = (3.56 \pm 0.21_{stat} \pm 0.28_{syst} \pm 0.43_{model}) \times 10^{-3} ,$$

with the dominant error coming from the modelling of the $b \to u l \nu_l$ decays.

A comparison of the different values of $|V_{ub}|$ is given on figure 14. All the values are in good agreement; and we see clearly that the results coming from the $\Upsilon(4S)$ experiments are dominated by the modelling error, while the results of the Z experiments are dominated by the statistical and systematic errors.

Considering all the other constraints [4] [11] on the unitarity triangle:

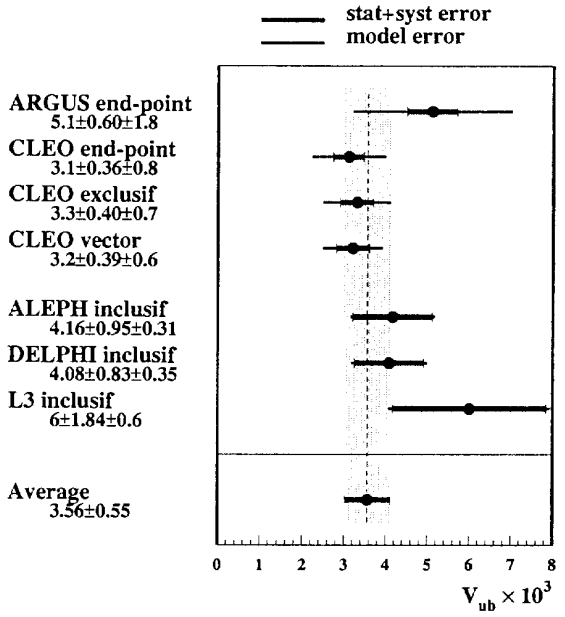

Figure 14: Comparison of the $|V_{ub}|$ measurements.

- $|\epsilon_K| = (2.280 \pm 0.013) \times 10^{-3}$ and $B_K = (0.75 \pm 0.15)$,
- $\Delta m_d = (0.471 \pm 0.016)\, ps^{-1} \Rightarrow |V_{td}| = (8.8 \pm 1.6)) \times 10^{-3}$,
- $\Delta m_s > 12.4\, ps^{-1} \Rightarrow \frac{|V_{ts}|}{|V_{td}|} > 4.2$ at 95 % C.L.;

one obtains the result presented on figure 15.

To conclude, these new results on the charmless semileptonic b hadron decays lead to an average value of the CKM matrix element (with 68 % of C.L. and with no gaussian error):

$$|V_{ub}| = (3.56 \pm 0.55) \times 10^{-3},$$

that is 15 % of accuracy.

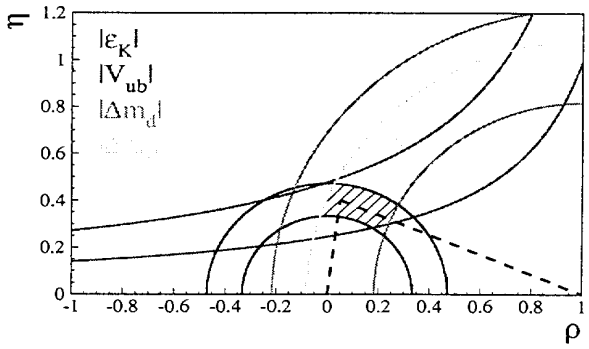

Figure 15: Constraints on the unitarity triangle, with the allowed region in hatched.

References

1. N. Cabibbo, Phys. Rev. Lett. 10 (1963) 531;
   M. Kobayashi and T. Maskawa, Prog. Theor. Phys. 42 (1973) 652;
2. L. Wolfenstein, Phys. Rev. Lett. 51 (1983) 233.
3. N. Uraltsev, Int. Jour. Mod. Phys. A11 (1996) 515;
   I. Bigi, R. Dikeman and N. Uraltsev, hep-ph/9706520.
4. A. Pich, Nucl. Phys. B (Proc. Suppl. WIN97) 66 (1998) 456;
   K. Berkelman, Nucl. Phys. B (Proc. Suppl. WIN97) 66 (1998) 447.
5. ARGUS Collaboration, Phys. Lett. B 234 (1990) 409;
   ARGUS Collaboration, Phys. Lett. B 255 (1991) 297;
   CLEO Collaboration, Phys. Rev. Lett. 64 (1990) 64;
   CLEO Collaboration, Phys. Rev. Lett. 71 (1993) 4111.
6. CLEO Collaboration, Phys. Rev. Lett. 70 (1993) 2681;
   CLEO Collaboration, Phys. Rev. Lett. 77 (1996) 5000.
7. CLEO Collaboration, ICHEP98 # 855.
8. ALEPH Collaboration, CERN-EP/98-067 (May 5, 1998), ICHEP98 # 933.
9. DELPHI Collaboration, ICHEP98 # 241.
10. L3 Collaboration, CERN-EP/98-097 (June 15, 1998), ICHEP98 # 561.
11. V. Andreev, *Oscillations of the B_d^0 mesons*, these proceedings;
    F. Parodi, *B_s mixing and limit on Δm_s*, these proceedings.